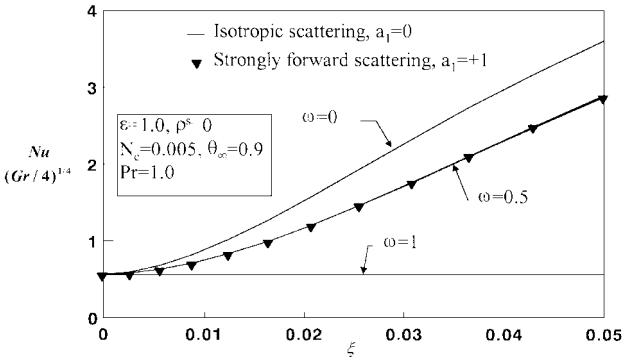

Fig. 2 Effect of scattering phase functions and albedo.

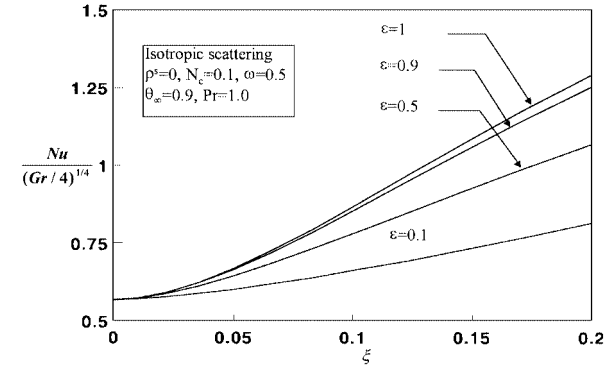

Fig. 3 Effect of emittance.

model. The single-scattering phase function for the LAS model is given as

$$p(\mu_p) = 1 + a_1 \mu_p$$

where μ_p is the cosine of the angle between the in-scattering and out-scattering directions: $a_1 = 0$ represents isotropic scattering, $a_1 = +1$ indicates strong forward scattering, whereas $a_1 = -1$ corresponds strong backward scattering. Forward scattering enhances the radiative transfer in the direction from the plate to fluid, whereas backward scattering retards the transfer. The slab phase function $p(\mu, \mu')$ required in Eqs. (8) and (9) can be easily obtained from $p(\mu_p)$[5].

The variation of $Nu/(Gr/4)^{1/4}$ with the dimensionless axial distance ξ is shown in Fig. 2. $Nu/(Gr/4)^{1/4}$ is seen to increase with ξ. The effect of degree of anisotropy a_1 is also presented in Fig. 2. For $a_1 = +1$, i.e., for strong forward scattering, the increase in $Nu/(Gr/4)^{1/4}$ over isotropic scattering is insignificant even at the low value of N_c, where radiation dominates over conduction. Strong backscattering ($a_1 = -1$) also affects only insignificant reduction in $Nu/(Gr/4)^{1/4}$. Increasing in scattering albedo decreases the heat flux as observed from Fig. 2. $\omega = 1$ yields the least heat flux because of the total decoupling of convective and radiative heat fluxes for this case. Figure 3 depicts the variation of heat flux with emittance. At higher emittances and ambient temperatures $Nu/(Gr/4)^{1/4}$ increases, and this is obvious because of larger radiation interactions.

Conclusion

Degree of radiation scattering anisotropy does not appear to affect the total heat flux from the plate to the fluid.

References

[1]Cess, R. D., "The Interaction of Thermal Radiation with Free Convection Heat Transfer," *International Journal of Heat Mass Transfer*, Vol. 9, No. 11, 1966, pp. 1269–1277.

[2]Arpaci, V. S., "Effect of Thermal Radiation on the Laminar Free Convection from a Heated Vertical Plate," *International Journal of Heat Mass Transfer*, Vol. 11, April 1968, pp. 871–881.

[3]Cheng, E. H., and Ozisik, M. N., "Radiation with Free Convection in an Absorbing, Emitting, and Scattering Medium," *International Journal of Heat Mass Transfer*, Vol. 15, No. 6, 1972, pp. 1243–1252.

[4]Ozisik, M. N., *Radiative Transfer and Interactions with Conduction and Convection*, Wiley, New York, 1973, pp. 249–312.

[5]Modest, M. F., *Radiative Heat Transfer*, McGraw–Hill, New York, 1993, pp. 312–315, 450–461, 541–571.

[6]Cheng, P., and Lui, H. C., "Planar Radiating Flow by the Method of Discrete Ordinates," *International Journal of Heat Mass Transfer*, Vol. 13, Oct. 1970, pp. 1793–1798.

[7]Love, T. J., and Grosh, R. J., "Radiative Heat Transfer in Absorbing, Emitting, and Scattering Media," *Journal of Heat Transfer*, Vol. 87, Series C, No. 2, 1965, pp. 161–166.

[8]Auer, L., "Acceleration of Convergence," *Numerical Radiative Transfer*, edited by W. Kalkofen, Cambridge Univ. Press, Cambridge, England, UK, 1987, pp. 101–109.

[9]Dennis, J. E., Jr., and Schnabel, R. B., *Numerical Methods for Unconstrained Optimization and Nonlinear Equations*, Prentice–Hall, Englewood Cliffs, NJ, 1983.

[10]Nachtsheim, P. R., and Swigert, "Satisfaction of Asymptotic Boundary Conditions in Numerical Solution of System of Nonlinear Equations of Boundary-Layer Type," NASA TN D-3004, 1965.

[11]Gear, C. W., *Numerical Initial Value Problems in Ordinary Differential Equations*, Prentice–Hall, Englewood Cliffs, New Jersey, 1971, pp. 136–168.

[12]Ostrach, S., "An Analysis of Laminar Free-Convection Flow and Heat Transfer About a Flat Plate Parallel to the Direction of the Generating Body Force," NACA TR-1111, 1953.

[13]Burmeister, L. C., *Convective Heat Transfer*, 2nd ed., Wiley, New York, 1993, p. 388.

Combined Convective and Radiative Heat Transfer in Turbulent Tube Flow

C. K. Krishnaprakas* and K. Badari Narayana†
ISRO Satellite Centre, Bangalore 560 017, India
and
Pradip Dutta‡
Indian Institute of Science, Bangalore 560 012, India

Nomenclature

d	= diameter of the tube, $2r_0$, m
f	= Darcy–Weissbach friction factor
g	= incident radiation function
h	= heat transfer coefficient, $q/(T_w - T_b)$, W/m^2-K
$I(\eta, \hat{s})$	= radiation intensity at distance η in the direction $\hat{s}$, W/m^2-sr
$I_b(T)$	= blackbody radiation intensity, W/m^2-sr
k	= thermal conductivity of the medium, W/m-K
N_c	= conduction-radiation number, $k\beta/4\sigma T_w^3$
Nu	= local Nusselt number, hd/k
$\hat{n}$	= normal vector to the surface
Pr	= Prandtl number, ν/α
Pr_t	= turbulent Prandtl number, $\varepsilon_m/\varepsilon_h$
$p(\hat{s}, \hat{s}')$	= scattering phase function
$p(\mu_p)$	= single-scattering phase function
q	= total heat flux by convection and radiation, W/m^2
Re	= Reynolds number, $u_b d/\nu$
r	= radial distance, m
r_0	= radius of the tube, m

Received 26 June 1998; revision received 20 October 1998; accepted for publication 8 March 1999.

*Engineer; currently Research Scholar, Indian Institute of Science, Bangalore 560 012, India.

†Head, Thermal Design Section, Thermal Systems Group.

‡Assistant Professor, Mechanical Engineering Department.

r^+ = dimensionless radius, $(ru_b/\nu)\sqrt{(f/8)}$
$\hat{s}$ = radiation direction vector
$\hat{s}_s$ = direction vector of the specularly reflected radiation from boundary
T = temperature, K
T_b = bulk mean temperature, $(2/r_0^2 u_b)\int_0^{r_0} uTr\,dr$, K
T_i = inlet fluid temperature, K
T_w = tube wall temperature, K
u = fluid flow velocity at radius r, m/s
u_b = bulk mean velocity of the fluid flow, $(2/r_0^2)\int_0^{r_0} ur\,dr$, m/s
u^+ = dimensionless velocity, $u/u_b\sqrt{(f/8)}$
w = dimensionless velocity, u/u_b
x = tube axial distance from the inlet, m
y = distance from wall, m
y^+ = dimensionless distance, $(yu_b/\nu)\sqrt{(f/8)}$
α = thermal diffusivity of the fluid, m^2/s
β = extinction coefficient, $\kappa+\gamma$, m^{-1}
γ = scattering coefficient, m^{-1}
ε = emittance of the tube surface
ε_h = thermal eddy diffusivity, m^2/s
ε_m = momentum eddy viscosity, m^2/s
ζ = direction cosine of $\hat{s}$ with the axis that is mutually orthogonal to radius vector and cylinder axis, $\sin\chi\sin\varphi$
η = dimensionless radius, r/r_0
θ = dimensionless temperature, T/T_w
κ = absorption coefficient, m^{-1}
μ = direction cosine of $\hat{s}$ with the radius vector, $\cos\chi\sin\varphi$
ν = kinematic viscosity of the fluid, m^2/s
ξ = dimensionless axial distance from the tube inlet, $(x/d)/(RePr)$
ρ = reflectance of boundary surface, $\rho^d+\rho^s=1-\varepsilon$
ρ^d = diffuse reflectance of boundary surface
ρ^s = specular reflectance of boundary surface
σ = Stefan–Boltzmann constant, $W/m^2\text{-}K^4$
υ = optical depth of the medium at radius $r=\int_0^r \beta\,dr$
υ_0 = optical thickness for radius r_0
χ = angle between $\hat{s}$ and cylinder axis
ψ = azimuthal angle of $\hat{s}$ in the plane perpendicular to cylinder axis
Ω = solid angle, sr
ω = scattering albedo, γ/β

Introduction

COMBINED forced convection and radiation heat transfer in absorbing, emitting, and scattering fluid flow through tubes is of interest in many engineering applications such as heat exchangers, furnaces, boilers, combustion chambers, rocket engines, solar collectors, cooling towers, nuclear reactors, etc. The radiative and convective heat fluxes are interdependent such that a change in heat flux in one mode affects heat flux in the other mode and vice versa. This means that the radiative transfer is coupled to the convective transfer and needs to be solved simultaneously. Mathematical formulation of the problem leads to a complicated nonlinear integrodifferential system, which is very difficult to solve. Wassel and Edwards[1] considered the radiation and laminar or turbulent convection interaction for a nongray fluid in a black-walled tube subjected to constant wall heat flux, using an exact treatment in terms of integral functions to evaluate the radiative flux. Balakrishnan and Edwards[2] investigated the effect of molecular gas radiation upon the thermal development downstream from a step change in wall temperature for both laminar and turbulent nongray fluid flow in a black-walled flat-plate duct. Chawla and Chan[3] solved the problem of thermally developing poiseuille flow with scattering using the method of collocation using splines. Azad and Modest[4] investigated the interaction of radiation with conduction and convection in thermally developing gray gas-particulate suspension flow through a circular tube using a modified differential approximation to solve the radiative transport, accounting diffuse reflection, and linear anisotropic scattering effects. Tabanfar and Modest[5] extended the interaction of thermal radiation with conduction and radiation for turbulent fluid flow to include nongray effects, but with black walls and constant surface heat flux using an exact treatment of radiative flux. Huang and Lin[6] studied the interaction of radiation with laminar convection in thermally developing circular pipe flow for absorbing and emitting gray fluid considering the axial radiative flux also. Chiou[7] studied the combined radiation-convection problem with nongray effects but with black walls. Yener and Ozisik[8] solved the simultaneous radiation and forced convection for an absorbing, emitting, and isotropically scattering thermally developing gray fluid flow inside a parallel-plate channel, employing Galerkin's method to solve the radiative transfer equation, which includes diffuse reflection effects also. Viskanta[9] has given recent reviews of the literature on radiation-convection interaction.

Combined convective and radiative heat transfer in turbulent fluid flow through a tube with constant surface temperature has not been studied earlier considering the effects of anisotropic scattering and diffuse/specular reflections from the wall. The present Note is concerned with the theoretical investigation of steady-state coupled forced hydrodynamically fully developed turbulent convection and radiation heat transfer in absorbing, emitting, and anisotropically scattering gray fluid flow through a constant surface temperature tube whose internal surface reflects radiation both diffusely and specularly. In the present Note the energy equation is solved by a finite difference method, and the radiation-transfer equation is solved by the method of discrete ordinates in conjunction with the Crank–Nicolson marching scheme.

Mathematical Model

Consideration is given to steady-state, combined forced convection, and radiation heat transfer in an absorbing, emitting, and anisotropically scattering gray fluid flowing through a circular tube of radius r_0. The flow is assumed to be hydrodynamically fully developed turbulent. The tube internal surface reflects radiation both diffusely and specularly. The assumption is made that the tube surface is gray, opaque, and isothermal.

Diffusive and radiative transfer in the axial direction is assumed to be negligible in comparison to that in the radial direction.[4] For the modeling of turbulent flow through ducts, the concept of eddy diffusivity is simple to use and has been found to be capable of accurately predicting the heat transfer behavior. In view of this, the eddy diffusivity concept is used for turbulence modeling. The energy equation for the medium may be written in dimensionless form as[4]

$$w\frac{\partial\theta}{\partial\xi}=\frac{4}{\eta}\frac{\partial}{\partial\eta}\left[\left(1+\frac{Pr}{Pr_t}\frac{\varepsilon_m}{\nu}\right)\eta\frac{\partial\theta}{\partial\eta}\right]-\frac{4(1-\omega)\upsilon_0^2}{N_c}[\theta^4-g(\eta)] \tag{1}$$

subject to the boundary conditions

$$\xi=0:\quad \theta=\theta_i,\qquad \eta=0:\quad \frac{d\theta}{d\eta}=0,\qquad \eta=1:\quad \theta=1 \tag{2}$$

The three-layer model describes the hydrodynamically established turbulent velocity profile for the fluid flow in the circular tube. In the laminar sublayer ($0<y^+<5$) and in the buffer layer ($5\le y^+\le 30$), the Von Karman equations are used and in the turbulent core ($y^+>30$) the Nikuradse equation modified by Reichardt is used[4,10]:

$$\begin{aligned} u^+&=y^+, && 0<y^+<5\\ u^+&=5.0\ell n y^+-3.05, && 5\le y^+\le 30\\ u^+&=2.5\ell n\left[\frac{1.5(1+\eta)}{(1+2\eta^2)}y^+\right]+5.5, && y^+>30 \end{aligned} \tag{3}$$

The velocity profile is evaluated such that the conservation of mass flow holds well. This is mathematically expressed as

$$\frac{4}{Rer_0^+}\int_0^{r_0^+} u^+r^+\,dr^+=1 \tag{4}$$

Equation (4) becomes a problem in finding r_0^+, which is related to f as $r_0^+ = Re\sqrt{(f/32)}$; therefore, f should be iteratively solved out from the implicit equation (4).

The two-layer model based on mixing-length theory is used for the momentum eddy diffusivity of fluid; the Van Driest–Spalding model for the wall region ($y^+ < 40$) and the Reichardt model for the turbulent core ($y^+ > 40$)[4] are

$$\frac{\varepsilon_m}{\nu} = \frac{k}{E}\left[e^{ku^+} - 1 - ku^+ - \frac{(ku^+)^2}{2} - \frac{(ku^+)^3}{6}\right], \qquad y^+ < 40 \tag{5}$$

$$\frac{\varepsilon_m}{\nu} = \frac{kr_0^+}{6}[1-\eta^2][1+2\eta^2], \qquad y^+ \geq 40$$

where the constants $k = 0.407$ and $E = 10.0$.

The diffusivity for heat is evaluated using the turbulent Prandtl-number concept. The earlier works on radiation interacting with forced turbulent convection either used $Pr_t = 1$ or a constant such as 0.85. Experimental evidence indicates that Pr_t has a sharp rise, in fact much higher than 1, in the sublayer, showing that the mechanisms of heat and momentum transfer differ greatly there.[10] Successful calculation of heat transfer rates critically depends on including the realistic variation of Pr_t along the radial direction of the tube. We, therefore, use a recent model for Pr_t known as *the extended Kays–Crawford model* to evaluate the turbulent Prandtl number[11]:

$$Pr_t = 1 \Bigg/ \left\{\frac{1}{2Pr_{t\infty}} + CPe_t\sqrt{\frac{1}{Pr_{t\infty}}} - (CPe_t)^2\left[1 - \exp\left(-\frac{1}{CPe_t\sqrt{Pr_{t\infty}}}\right)\right]\right\} \tag{6}$$

$$Pe_t = Pr\frac{\varepsilon_m}{\nu}, \qquad Pr_{t\infty} = 0.85 + \frac{D}{PrRe^{0.888}}$$

$$C = 0.3, \qquad D = 100$$

In Eq. (1), $g(\eta)$ is the dimensionless incident radiation function evaluated from the radiation intensity distribution $I(\eta, \hat{s})$ as[12]

$$g(\eta) = \frac{1}{4\sigma T_w^4}\int_{4\pi} I(\eta, \hat{s})\, d\Omega \tag{7}$$

$I(\eta, \hat{s})$ is evaluated from the solution of radiation transfer equation (RTE) together with the boundary conditions, which are given as

$$\frac{\mu}{\upsilon_0}\frac{\partial I(\eta,\hat{s})}{\partial \eta} + \frac{\zeta}{\upsilon_0 \eta}\frac{\partial I(\eta,\hat{s})}{\partial \psi} + I(\eta,\hat{s}) = (1-\omega)I_b(\eta) + \frac{\omega}{4\pi}\int_{4\pi} I(\eta,\hat{s}')p(\hat{s},\hat{s}')\, d\Omega' \tag{8}$$

$$I(\eta=1,\hat{s}) = \varepsilon I_b(T_w) + \frac{\rho^d}{\pi}\int_{\hat{n}\cdot\hat{s}'<0} I(\eta=1,\hat{s}')|\hat{n}\cdot\hat{s}'|\, d\Omega' + \rho^s I(\eta=1,\hat{s}_s) \tag{9}$$

$$I(\eta=0,\hat{s}) = I(\eta=0,-\hat{s}) \tag{10}$$

The total radial heat flux $q(\xi)$ at the tube wall surface, which is the sum of the conduction and the radiation contributions, may be expressed in terms of a local Nusselt number, which is defined as

$$Nu(\xi) = \frac{q(\xi)d}{k[T_w - T_b(\xi)]} \tag{11}$$

This may be expressed in terms of dimensionless quantities as

$$Nu = \frac{1}{(\theta_b - 1)}\left[-2\frac{d\theta}{d\eta}\bigg|_{\eta=1} + \frac{\upsilon_0}{4N_c}\psi_r\right] \tag{12}$$

where $\theta_b = T_b/T_w$ is the dimensionless bulk mean temperature and

$$\psi_r = \frac{\int_{4\pi} I[\upsilon(\eta=1),\hat{s}]\hat{n}\cdot\hat{s}\, d\Omega}{\sigma T_w^4} \tag{13}$$

Numerical Scheme

To obtain the temperature and the radiation intensity distributions, the energy equation, Eq. (1), and the RTE, Eq. (8), are to be solved simultaneously. We adopt a numerical iterative procedure in which the derivatives with respect to η in the energy equation are replaced by second-order finite differences, and this leads to a system of nonlinear coupled ordinary differential equations describing the variation of nodal temperatures with the independent variable ξ (Ref. 13). The system of ordinary differential equations is solved with the Crank–Nicolson method.[14] Because for turbulent flow the velocity profile changes rapidly in the vicinity of the boundary, it is necessary to adopt a nonuniform mesh with a finer discretization near the tube surface and a coarser grid away from it. Robert's coordinate stretching function was used for the coordinate transformation to accomplish nonuniform mesh.[13] Calculating the nodal temperatures for the next ξ step involves the unknown $g(\eta)$ at that step. Therefore, first a temperature distribution $\theta(\eta)$ is assumed, the RTE is solved to obtain the $I(\eta, \hat{s})$ distribution, $g(\eta)$ profile is evaluated from Eq. (7), and then θ is solved for the next step. This process involves a nonlinear system in θ, which is solved by the Newton–Raphson method. The preceding numerical scheme is repeated until convergence, i.e., the maximum norm of the relative difference of the intensity and temperature distributions between two successive iterations falls below 1.0E−4. The whole numerical procedure is repeated for all of the downstream positions. The RTE is solved by the discrete ordinates method (DOM).[12] DOM converts the integrodifferential equation and the boundary conditions, Eqs. (8–10), into a two-point boundary-value problem in ordinary differential equations that are solved by a variant of the shooting method in conjunction with the Crank–Nicolson scheme as the core integrator.[14] The implicit equation (4) was solved numerically using the method of regula-falsi.

Results and Discussion

To investigate the effect of anisotropic scattering in heat transfer, we consider a linear anisotropic scattering (LAS) model. The single-scattering phase functions $p(\mu_p)$ for the LAS model for various cases are given next, where μ_p is a cosine of the angle between the in-scattering and out-scattering directions. The phase function $p(\hat{s}, \hat{s}')$ required in Eq. (8) can be easily obtained from $p(\mu_p)$ (Ref. 12).

Isotropic scattering:

$$p(\mu_p) = 1$$

Forward linear anisotropic scattering:

$$p(\mu_p) = 1 + P_1(\mu_p)$$

Backward linear anisotropic scattering:

$$p(\mu_p) = 1 - P_1(\mu_p)$$

The numerical accuracy of the computer algorithms is validated by comparing the values of the convective Nusselt numbers from the present analysis with the exact analytical results for laminar tube flow and experimental correlation for turbulent tube flow. The calculated laminar Nusselt numbers were within 0.5% of the exact results presented by Kays and Crawford (p. 133 of Ref. 10). For the comparison of turbulent flow results, the well-known Dittus–Boelter correlation as interpreted by Kakac et al.[15] and given in Kays and Crawford (p. 319 of Ref. 10) is used, i.e., $Nu = 0.024Re^{0.8}Pr^{0.4}$ for heating. The calculated asymptotic turbulent Nusselt numbers were higher than the Dittus–Boelter values, and the difference was within 6% for many values of turbulent Reynolds numbers in the range 10^4–10^5 and $Pr = 1$. This kind of deviation in results between theoretical values and experimental correlations for turbulent flow analysis is expected in view of the models used for eddy momentum

diffusivity and turbulent Prandtl number and is quite acceptable for engineering calculations.

The radiation model was separately validated by comparing the heat flux results for the cases of 1) a gray, nonscattering, and isothermal cylinder and 2) a gray, isotropically scattering medium between two concentric cylinders at radiative equilibrium with that presented in Modest (pp. 475, 476 of Ref. 12). For both the cases exact solutions in terms of integral formulations are available. The results from the present model were in good agreement with the exact results in the sense that the difference was less than 2%. For larger optical thickness the difference was even less.

Figure 1 depicts the local Nusselt number as a function of dimensionless distance from the tube inlet for various values of optical thickness. The Nusselt number increases with increasing optical thickness of the medium. As ω increases, the Nusselt number is seen to be decreasing as seen from Fig. 2 because of radiation getting decoupled from the other modes of heat transfer as scattering albedo increases [see Eq. (1)]. From the figures one can see that for radiating flow of a heating fluid the Nusselt number has a minimum at a certain downstream position, and this position shifts toward the inlet as the radiative contribution increases. This happens because of the continuous reduction in convective heat flux and augmentation of radiative flux as it moves away from the inlet. From Fig. 3 one

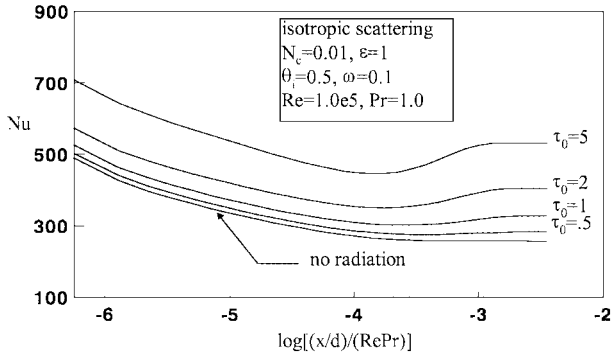

Fig. 1 Local Nusselt number: effect of optical thickness τ_0.

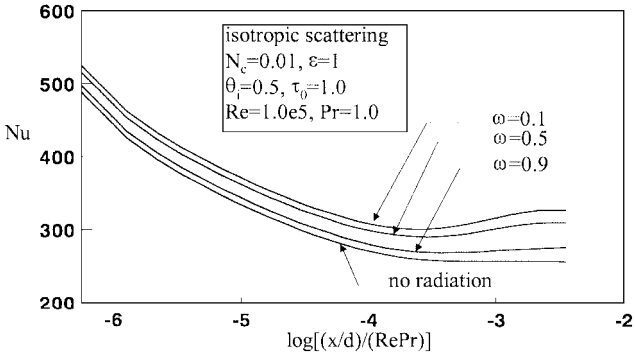

Fig. 2 Local Nusselt number: effect of scattering albedo ω.

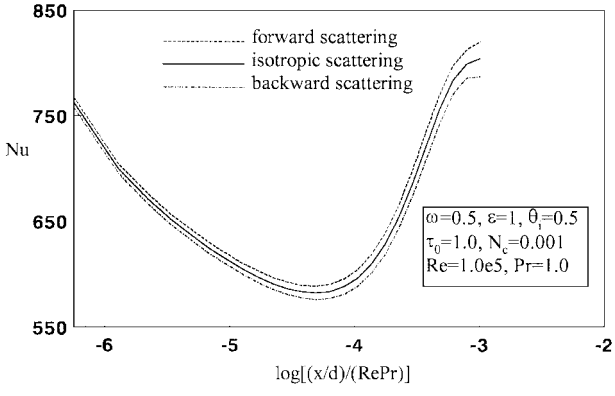

Fig. 3 Local Nusselt number: effect of scattering phase functions.

Table 1 Local Nusselt number for diffuse ($\rho^s = 0$, $\rho = \rho^d$) and specular ($\rho^d = 0$, $\rho^s = \rho$) reflection cases[a]

	Nu			
	$\omega_0 = 0.1$		$\omega_0 = 1.0$	
$\log[(x/d)/(RePr)]$	Diffuse	Specular	Diffuse	Specular
−5.5	379.52	379.47	422.37	422.10
−5.0	339.89	339.83	383.14	382.71
−4.5	303.78	303.71	348.35	347.49
−4.0	273.50	273.39	323.65	321.61
−3.5	262.49	262.33	326.05	322.29
−3.0	262.52	262.26	362.64	356.15
−2.9	262.92	262.64	370.16	363.38
−2.8	263.31	262.99	375.41	368.53
−2.7	263.62	263.24	377.80	370.97

[a]Isotropic scattering: $Re = 1.0e5$, $Pr = 1$, $N_c = 0.001$, $\varepsilon = 0.1$, $\theta_i = 0.5$, $\omega = 0.1$.

can see that strongly backward scattering gives the lowest heat flux results, strongly forward scattering gives the highest heat fluxes, and isotropic scattering gives an intermediate result. A reduction in N_c is seen to cause an increase in Nusselt number, and this is expected in view of radiation dominance in such cases. An increase in emittance increases the Nu in view of the enhanced radiative flux. Another interesting result noted from Table 1 is that a tube with fully specularly reflecting surface ($\rho^d = 0$, $\rho^s = \rho$) always transfers less heat than a tube with fully diffusely reflecting ($\rho^s = 0$, $\rho^d = \rho$) surface. This difference diminishes as ω and N_c increases or optical thickness decreases. However, diffuse and specular results do not show any appreciable deviation.

The results discussed in this Note are based on the application of the S_6 method.[12] Increasing S_6 quadrature to S_8 resulted in only less than 0.5% change in Nu results. All of the computations were carried out on a Pentium-processor-based PC. The average CPU time per run is about 10 s.

Conclusions

The effect of anisotropy is significant for low conduction-radiation numbers and high values of scattering albedo. Strongly forward scattering media transfers more heat than isotropic or backward scattering media.

Specularly reflecting tube wall transfers less heat than diffusely reflecting tube wall. The effect is pronounced at larger distances from the inlet for low values of N_c and ε and high ω_0.

References

[1]Wassel, A. T., and Edwards, D. K., "Molecular Gas Radiation in a Laminar or Turbulent Pipe Flow," *Journal of Heat Transfer*, Vol. 98, No. 1, 1976, pp. 101–107.

[2]Balakrishnan, A., and Edwards, D. K., "Molecular Gas Radiation in the Thermal Entrance Region of a Duct," *Journal of Heat Transfer*, Vol. 101, No. 3, 1979, pp. 489–495.

[3]Chawla, T. C., and Chan, S. H., "Combined Radiation Convection in Thermally Developing Poiseuille Flow with Scattering," *Journal of Heat Transfer*, Vol. 102, No. 2, 1980, pp. 297–302.

[4]Azad, F. H., and Modest, M. F., "Combined Radiation and Convection in Absorbing, Emitting and Anisotropically Scattering Gas-Particulate Tube Flow," *International Journal of Heat Mass Transfer*, Vol. 24, No. 10, 1981, pp. 1681–1698.

[5]Tabanfar, S., and Modest, M. F., "Combined Radiation and Convection in Absorbing, Emitting Nongray Gas-Particulate Tube Flow," *Journal of Heat Transfer*, Vol. 109, No. 2, 1987, pp. 478–484.

[6]Huang, J. M., and Lin, J. D., "Radiation and Convection in Circular Pipe with Uniform Wall Heat Flux," *Journal of Thermophysics and Heat Transfer*, Vol. 5, No. 4, 1991, pp. 502–507.

[7]Chiou, J. S., "Combined Radiation-Convection Heat Transfer in a Pipe," *Journal of Thermophysics and Heat Transfer*, Vol. 7, No. 1, 1993, pp. 178–180.

[8]Yener, Y., and Ozisik, M. N., "Simultaneous Radiation and Forced Convection in Thermally Developing Turbulent Flow Through a Parallel-Plate Channel," *Journal of Heat Transfer*, Vol. 108, No. 4, 1986, pp. 985–988.

[9]Viskanta, R., "Radiation Transfer: Interaction with Conduction and Convection and Approximate Methods in Radiation," *Proceedings of the Seventh International Heat Transfer Conference*, Vol. 1, Hemisphere, Washington, DC, 1982, pp. 103–121.

[10] Kays, W. M., and Crawford, M. E., *Convective Heat and Mass Transfer*, 3rd ed., McGraw–Hill, New York, 1993.
[11] Weigand, B., Ferguson, J. R., and Crawford, M. E., "An Extended Kays and Crawford Turbulent Prandtl Number Model," *International Journal of Heat and Mass Transfer*, Vol. 49, No. 17, 1997, pp. 4191–4196.
[12] Modest, M. F., *Radiative Heat Transfer*, McGraw–Hill, New York, 1993.
[13] Ozisik, M. N., *Finite Difference Methods in Heat Transfer*, CRC Press, Boca Raton, FL, 1994.
[14] Hall, G., and Watt, J. M. (eds.), *Modern Numerical Methods for Ordinary Differential Equations*, Clarendon, Oxford, 1976.
[15] Kakac, S., Shah, R. K., and Aung, W., *Handbook of Single-Phase Convective Heat Transfer*, Wiley, New York, 1987.

Estimation of Wall Heat Flux in an Inverse Convection Problem

Hung-Yi Li* and Wei-Mon Yan†
Hua Fan University,
Taipei 22305, Taiwan, Republic of China

Introduction

In the inverse heat conduction problems, the surface conditions or the thermal properties of a material are estimated by utilizing the temperature measurements within the medium. These problems have received much attention and numerous papers have been devoted to this topic of research. Inverse radiation problems have also been investigated extensively. They are concerned with the determination of the radiative properties or the internal temperature profile of a medium from the measured radiation data. Despite the relatively large interest given in the inverse problems of heat conduction and radiation, only a small amount of work is available for the inverse heat convection problems.[1–3] In all of these studies, the unknown functions to be estimated are of one variable for the inverse convection problems. In this Note, we consider the estimation of the space- and time-dependent wall heat flux for unsteady laminar-forced convection between parallel flat plates from the temperature measurements taken inside the flow or at the opposite wall.

Analysis

Direct Problem

Consider unsteady laminar-forced convection heat transfer in a parallel plate duct with channel width b. The flow enters the channel with a fully developed velocity distribution $u(y)$ and a constant temperature T_0. Initially, the duct walls are kept thermally insulated. At time $t = 0$, the thermal condition of the upper wall at $y = b$ is suddenly changed and is subjected to wall heating condition with a function of position x and time t. The flow is assumed to have constant properties and the buoyancy term is neglected. It is intended to provide a first step toward future work, in which these effects will be considered. Figure 1 describes the geometry and coordinates. By introducing the following dimensionless quantities:

$$X = x/bPe, \qquad Y = y/b, \qquad \upsilon = \alpha t/b^2$$
$$\theta = k(T - T_0)/bq_{\text{ref}}, \qquad Pe = \bar{u}b/\alpha, \qquad U = u/\bar{u} \quad (1)$$
$$Q = q/q_{\text{ref}}, \qquad U = \tfrac{3}{2}[1 - (2Y - 1)^2]$$

where k is the thermal conductivity, α is the thermal diffusivity, T is the temperature, q is the wall heat flux, q_{ref} is the reference heat flux, and $\bar{u}$ is the mean velocity. The governing energy conservation equation in dimensionless form for the problem is given by

$$\frac{\partial\theta}{\partial\upsilon} + U\frac{\partial\theta}{\partial X} = \frac{\partial^2\theta}{\partial Y^2} \quad (2a)$$

with the initial condition and the boundary conditions

$$\theta(X, Y, 0) = 0 \quad (2b)$$
$$\theta(0, Y, \upsilon) = 0 \quad (2c)$$
$$\frac{\partial\theta(X, 0, \upsilon)}{\partial Y} = 0 \quad (2d)$$
$$-\frac{\partial\theta(X, 1, \upsilon)}{\partial Y} = Q(X, \upsilon) \quad (2e)$$

Inverse Problem

In the direct problem, the velocity distribution, the initial condition, and the boundary conditions are given to determine the temperature distribution in the flowfield. In the inverse problem, the temperature data are assumed to be measured inside the flow or at the lower wall. The dimensionless heat flux at the upper wall, $Q(X, \upsilon)$, is recovered by using the measured data. The estimation of the wall heat flux from the knowledge of the measured temperature data can be constructed as a problem of minimization of the objective function:

$$J = \sum_{i=1}^{M}\sum_{k=1}^{N}(\theta_{i,k} - Z_{i,k})^2 \quad (3)$$

where $\theta_{i,k} = \theta(X_i, Y_1, \upsilon_k)$ is the calculated dimensionless temperature for an estimated $Q(X, \upsilon)$, and $Z_{i,k} = Z(X_i, Y_1, \upsilon_k)$ is the measured dimensionless temperature. If $Y_1 = 0$, the measurements are taken at the lower wall; if $0 < Y_1 < 1$, the measurements are taken inside the fluid. M and N are the numbers of the measured points in the X and υ directions, respectively.

In this Note, the conjugate gradient method[4] is employed to determine the unknown wall heat flux $Q(X, \upsilon)$ by minimizing the objective function J. The iterative process is

$$Q^{p+1}_{m,n} = Q^{p}_{m,n} - \beta^p d^p_{m,n} \quad (4)$$

where $Q_{m,n} = Q(X_m, \upsilon_n)$, β^p is the step size, and $d^p_{m,n}$ is the direction of descent, which is determined from

$$d^p_{m,n} = \left(\frac{\partial J}{\partial Q_{m,n}}\right)^p + \gamma^p d^{p-1}_{m,n} \quad (5)$$

and the conjugate coefficient γ^p is computed from

$$\gamma^p = \sum_{m=1}^{M}\sum_{n=1}^{N}\left[\left(\frac{\partial J}{\partial Q_{m,n}}\right)^p\right]^2 \Bigg/ \sum_{m=1}^{M}\sum_{n=1}^{N}\left[\left(\frac{\partial J}{\partial Q_{m,n}}\right)^{p-1}\right]^2$$
$$\text{with} \qquad \gamma^0 = 0 \quad (6)$$

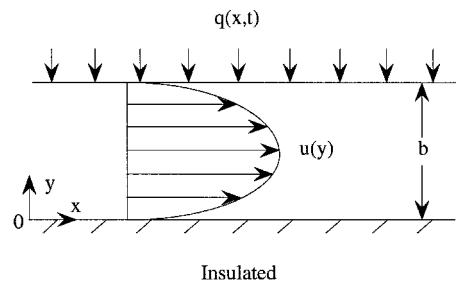

Fig. 1 Geometry and coordinates.

Received 8 July 1998; revision received 19 November 1998; accepted for publication 23 November 1998.

*Professor, Department of Mechanical Engineering, Shihtin; hyli@huafan.hfu.edu.tw.
†Professor, Department of Mechanical Engineering, Shihtin.